

# Solvent Vapor Annealing and Plasma Treatment Stabilize Silver Nanowire Layers

Thilo Grammes,\* Johannes Maurer, Lola González-García, and Tobias Kraus

Silver nanowires (AgNW) find use in transparent conductive electrodes with applications in solar cells, touch screens, and wearables. Unprotected AgNW are prone to atmospheric corrosion and lose conductivity over time. Known passivation techniques either require submersion of pre-deposited AgNW in liquid compounds or the modification of AgNW inks prior to deposition, which alters viscosity and complicates deposition. Here, new possibilities for stabilization of pre-deposited AgNW networks without need for submersion are explored. It is demonstrated that AgNW networks can be stabilized either by argon or hydrogen plasma treatment or by solvent vapor annealing with ethanol, methanol, or ethyl acetate. These treatments yielded stable electrical resistance over at least nine weeks, whereas untreated or thermally annealed AgNW layers quickly lost conductivity. The potential of solvent vapor annealing is further explored by demonstrating a new processing technique for stable polymer matrix composites containing AgNW. Co-deposited layers of AgNW with polystyrene microbeads are annealed in ethyl acetate vapor to stabilize the AgNW while at the same time merging polymer beads into a closed film around the AgNW. The resulting composites maintained stable resistance and transmittance for at least seven weeks.

## 1. Introduction

Transparent conductive materials are of key importance for the development of solar cells,<sup>[1–3]</sup> touch screens,<sup>[4]</sup> and organic light emitting diodes.<sup>[5]</sup> The currently predominant materials in this field are transparent conductive oxides, among which indium tin oxide (ITO) found most widespread use.<sup>[2,6]</sup> These ceramic materials are brittle and their expensive, vacuum-based production renders coating over larger areas difficult.<sup>[7,8]</sup> The high temperatures during processing can damage polymer substrates, which are required for flexible electrodes.<sup>[7,9,10]</sup> Silver nanowires (AgNW) have found attention as an alternative to ITO. They are synthesized at relatively low cost<sup>[7,11,12]</sup> and can be deposited by solution processes such as spray, spin, dip, or rod coating or filtration,<sup>[13–16]</sup> thus rendering them viable for electrode printing. AgNW meshes provide conductivity by forming conductive percolating networks<sup>[7,9]</sup> while offering

competitive transparency,<sup>[13,17,18]</sup> including higher infrared transparency than ITO.<sup>[7]</sup>

As a drawback, silver nanowires are prone to corrosion by sulphidation.<sup>[19,20]</sup> In a pioneering corrosion study, Elechiguerra et al.<sup>[19]</sup> exposed silver nanowires and nanoparticles covered with ligands of polyvinylpyrrolidone (PVP) to air for up to 24 weeks. The nanowires formed core-shell structures with silver sulphide covering the original geometry. Similar core-shell structures were reported by Levard et al.<sup>[20]</sup> who exposed silver nanoparticles to H<sub>2</sub>S solution. Both studies pointed out that the widely-used PVP ligand shell does not protect AgNW against corrosion,<sup>[19,20]</sup> which increases sheet resistance and decreases optical transmittance over time.<sup>[14,18]</sup> Im et al.<sup>[14]</sup> exposed AgNW and composites of AgNW in UV-curable resin to H<sub>2</sub>S solution and demonstrated a high increase in sheet resistance after only few minutes. After annealing AgNW at 250 °C for 6 h they also found silver oxide and noted increasing sheet resistance and decreasing transmittance. Short thermal annealing is a common practice to reduce the sheet resistance by removing polymeric ligands and sintering AgNW junctions,<sup>[21]</sup> but without further protective measures it does not increase the long-term stability of the resulting AgNW layers.<sup>[14]</sup>

Many protective measures that have been explored so far complicate processing by introducing additional coating steps. Early attempts included covering the AgNW with metal oxides<sup>[22]</sup>

T. Grammes, J. Maurer, L. González-García, T. Kraus  
INM – Leibniz Institute for New Materials  
Campus D2 2, 66123 Saarbrücken, Germany  
E-mail: [thilo.grammes@partner.kit.edu](mailto:thilo.grammes@partner.kit.edu)

T. Grammes  
Institute for Applied Materials  
Karlsruhe Institute of Technology (KIT)  
Hermann-von-Helmholtz-Platz 1, 76344 Eggenstein-Leopoldshafen,  
Germany

L. González-García  
Department of Materials Science and Engineering  
Saarland University  
Campus D2 2, 66123 Saarbrücken, Germany

T. Kraus  
Colloid and Interface Chemistry  
Saarland University  
66123 Saarbrücken, Germany

 The ORCID identification number(s) for the author(s) of this article can be found under <https://doi.org/10.1002/ppsc.202400091>

© 2024 The Author(s). Particle & Particle Systems Characterization published by Wiley-VCH GmbH. This is an open access article under the terms of the [Creative Commons Attribution](https://creativecommons.org/licenses/by/4.0/) License, which permits use, distribution and reproduction in any medium, provided the original work is properly cited.

DOI: 10.1002/ppsc.202400091

or graphene oxide,<sup>[23,24]</sup> but this involved sophisticated additional coating steps, and the graphene oxide still allowed for corrosion, albeit more slowly. More successful coating approaches included spin coating AgNW layers with the conductive polymer poly(3,4-ethylenedioxythiophene):poly(styrenesulfonate) (PEDOT:PSS)<sup>[25]</sup> or with chitosan.<sup>[3]</sup> Other groups attempted passivation of AgNW prior to deposition, without an additional coating step. Idier et al.<sup>[18]</sup> added triphenylphosphine<sup>[18]</sup> to a silver nanowire suspension in isopropanol and achieved sheet resistances of below 50  $\Omega$  sq<sup>-1</sup> and a transmittance of 80% at 550 nm after 110 days in room temperature atmosphere. Wang et al.<sup>[26]</sup> reported similar sheet resistance as well as transmittance between 85 and 95% after 300 days for composites fabricated from an aqueous dispersion of AgNW to which they added a solution of chitosan and lactic acid. Although this one-step approach with passivated AgNW in the ink is attractive regarding simplified processing, dissolved chitosan polymer in the ink in the latter example increases ink viscosity and causes wetting issues,<sup>[26]</sup> rendering the coating of larger areas difficult. As an alternative, AgNW can be chemically passivated without a covering polymer layer by immersing AgNW networks in organic acids carrying mercapto groups (-SH).<sup>[15,16]</sup> The thiols replace the PVP ligand and block the AgNW surface. Surface silver atoms are held in place in a state similar to sulphidation, thus reducing the driving force for corrosion by sulphur components in the air. Such chemical passivation yielded AgNW layers with sheet resistance/transmittance at 550 nm of about 20  $\Omega$  sq<sup>-1</sup>/70% (ambient air),<sup>[16]</sup> and 20–30  $\Omega$  sq<sup>-1</sup>/85–90% (climate chamber 85 °C, 85% RH),<sup>[15]</sup> respectively, after 120 days. However, this passivation by mercapto groups still involves an immersion step, which may disturb the arrangement of previously deposited AgNW layers.

We aim here to explore alternative stabilizing treatments for pre-deposited AgNW layers, assuming that the aforementioned submerging step for passivation can be replaced by a suitable treatment of AgNW layers with plasma or vapor to avoid disturbing the arrangement of AgNW. We exposed drop casted AgNW layers to plasma treatment with argon or hydrogen plasma, and to solvent vapor annealing (SVA) with readily available solvents (ethanol, methanol, and ethyl acetate) and found that both approaches have a stabilizing effect on electrical resistance when compared to untreated or thermally annealed AgNW. We investigated the origin of this effect by means of transmission electron microscopy (TEM) and a reference ageing experiment in argon atmosphere. By contrast to aforementioned techniques, this stabilization of AgNW by plasma or vapor enables simple colloid-based fabrication of stabilized AgNW layers without the need to expose the AgNW layers to a liquid phase after deposition. This opens up new possibilities for further processing of AgNW layers.

We recognize engineering potential that lies in the stabilization by solvent vapor annealing: If AgNW are co-deposited with colloidal polymer microbeads, a suitable solvent vapor may at the same time stabilize the AgNW and fuse the polymer beads into a closed film. We demonstrate the feasibility of this approach by creating composites of AgNW embedded in a polystyrene (PS) film. We drop casted aqueous suspensions containing AgNW and colloidal polystyrene microbeads that form self-assembled mono- or multilayers without the viscosity issues that come with poly-

mer solutions.<sup>[27,28]</sup> We then used solvent vapor annealing with ethyl acetate vapor to transform the PS particle layer into a closed film around the AgNW.

The practice of embedding AgNW in a polymer matrix is common to reduce electrode roughness and to improve mechanical stability. But so far, this embedding usually was achieved either by pressing<sup>[29]</sup> or by coating the AgNW with a polymer solution.<sup>[17,25,30–33]</sup> Most polymer deposition steps may substantially alter the arrangement of the AgNW layer and they involve the challenging handling of viscous polymer solutions. Our new approach avoids this, since colloidal polymer microbeads can be co-deposited with AgNW in an aqueous solution.

We note that there are only few studies on the long-term stability of AgNW-polymer composite layers. Only one evaluated the long-term stability over several months,<sup>[25]</sup> two evaluated short-term ageing over two weeks or less.<sup>[14,15]</sup> The available data on long-term stability is therefore limited, yet stability is indispensable for the practical application of such composites. We compared the stability of electrical resistance for non-embedded AgNW and AgNW/PS composites created by solvent vapor annealing as described above and found a stabilising effect of the vapor treatment in both cases. Lastly, we explored a more scalable, homogeneous deposition route of our composites by a moving meniscus approach and evaluated the electrical and optical stability over seven weeks.

## 2. Experimental Section

### 2.1. Raw Materials

The commercial silver nanowires (AgNW-130 from Seashell Technology, La Jolla, USA) used for this study were delivered as a suspension with 2.5 wt.% solid content in isopropanol. The wires had an average diameter of 130 nm and an average length of 35  $\mu$ m, according to manufacturer, and were covered with a ligand shell of PVP. For composite processing, commercial, monodisperse polystyrene microbeads (Polybead from Polysciences Europe, Hirschberg an der Bergstraße, Germany) were used. The beads had a diameter of 1  $\mu$ m (in one experiment 45  $\mu$ m) and were delivered as a suspension of 2.5 wt.% in deionized water.

### 2.2. Deposition and Annealing

**Figure 1** provides an overview of the preparation steps for deposition and treatment of AgNW layers (**Figure 1a**) as well as AgNW/PS composite layers (**Figure 1b**). AgNW networks were prepared by drop casting 20  $\mu$ L of AgNW suspension onto a standard soda-lime glass substrate (**Figure 1a**). The samples were stored in laboratory air for up to 9 weeks. Electrical resistance was measured regularly during that time. Untreated AgNW layers were prepared as reference, to be compared with AgNW layers that underwent thermal annealing, solvent vapor annealing, or plasma treatment as detailed below. Three samples were prepared for each type.

Thermal annealing was done by mounting the samples onto a heating plate pre-heated to 150 °C for 30 min (**Figure 1a**). Solvent vapor annealing was performed by exposing the samples to

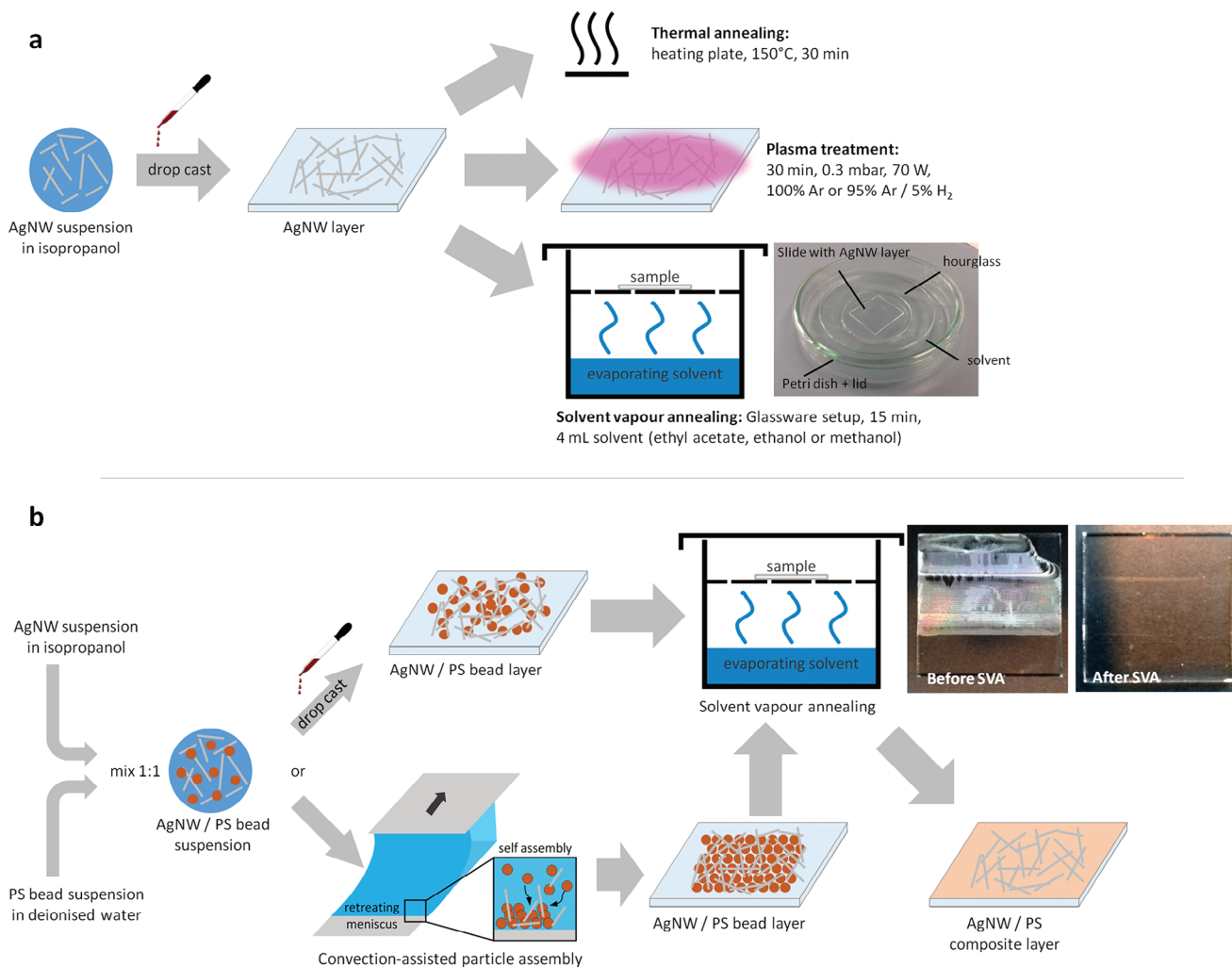


**Figure 1.** Schematic preparation steps for layer deposition and subsequent treatment. a) Drop casting of AgNW layer and treatment with either thermal annealing, plasma treatment or solvent vapor annealing. Inset photograph shows glassware setup for SVA. b) Deposition of AgNW/PS bead layer either by drop casting or convection-assisted particle assembly and subsequent solvent vapor annealing to form AgNW/PS composite layer. Inset photographs show PS microbead layers sizing 20 × 20 mm<sup>2</sup> before (opaque) and after SVA (transparent).

laboratory-grade methanol, ethanol, or ethyl acetate for 15 min. Here, a simple setup was created using laboratory glassware (see photograph inset in Figure 1a). An initial solvent amount of 4 mL was placed in a petri dish. An hourglass carrying the samples was added, preventing direct contact between sample and liquid solvent. Then, the petri dish was closed with a lid to expose the samples to the evaporating solvent. Plasma treatment was performed for 30 min either with pure argon or with a mixture of 5 vol% hydrogen in argon in a low-pressure plasma reactor (RF PICO, Diener electronic, Ebhausen, Germany), using a power of 70 W and a pressure of 0.3 mbar, where the gas temperature remained below 35 °C.

To prepare composites of AgNW in a polystyrene matrix, AgNW and PS microbeads were co-deposited on a glass substrate (Figure 1b) by using either drop casting an ink containing equal weight fractions of AgNW and PS microbead suspensions or by convection-assisted particle assembly (CAPA)<sup>[27,28,34]</sup> using the same ink on a dedicated setup. For CAPA, glass sub-

strates were positioned on a translational stage (PLS-85 from PI miCos, Eschbach, Germany). The stage was mounted on a microscope (AXIO from ZEISS, Oberkochen, Germany) for in situ observation and parameter adjustment. Approximately 50 µL of the AgNW/PS ink were injected using a syringe to fill the gap between the substrate and a glass blade placed about 0.5 mm above the substrate. The blade was moved over the substrate at 50 µm s<sup>-1</sup> to create a meniscus that travelled over the substrate. The colloidal particles assembled in the resulting thin liquid film. The CAPA process was performed without additional heating in an air-conditioned laboratory at 20 °C and 50–70% relative humidity.

All glass substrates were cleaned and treated with oxygen plasma (same conditions as plasma treatment above) for 5 min to create a hydrophilic surface and ensure good wetting for layer deposition.

The deposited films of AgNW and PS beads were transformed into AgNW/PS composite films by solvent vapor annealing with

laboratory-grade ethyl acetate, using the same parameters as above (Figure 1b). Three composite samples were prepared for the drop casting and the CAPA approach, respectively.

In order to assess the long-time performance of these composites, the samples were stored in laboratory air for up to 7 weeks. The specular UV–vis transmittance and the sheet resistance were measured regularly during that time.

### 2.3. Electrical Resistance

Electrical resistance measurements were carried out with the two-point method using a multimeter (Votcraft VC160 from Conrad Electronic, Hirschau, Germany). Parallel stripes of silver paint were applied as contacts (with negligible contact resistance) on two edges of rectangular samples with an area  $w$  times  $l$ , where  $l$  is the distance and  $w$  is the width of the film between the contacts. The sheet resistance  $R_{sq}$  was calculated from the measured resistance  $R$  as:

$$R_{sq} = R \cdot \frac{w}{l} \quad (1)$$

### 2.4. UV–vis Spectroscopy

Specular transmittance was characterized by UV–vis spectroscopy (Cary 5000 from Agilent Technologies, Waldbronn, Germany) against an air reference in a wavelength range from 350 to 800 nm. The transmittance reported here deliberately compounds layer and substrate properties to include the transmittance losses due to reflection at an unmodified layer-substrate boundary.

### 2.5. Electron Microscopy

Scanning electron microscopic (SEM) analysis of drop-casted AgNW layers after different treatments was done on an ESEM Quanta 400 FEG (FEI, Hillsboro, USA) operating in high vacuum, with an acceleration voltage of 20 kV.

Additional untreated, solvent-vapor annealed (ethyl acetate), and Ar plasma treated AgNW films were prepared on TEM grids by drop casting and subsequent annealing (same parameters as above). They were analyzed with a TEM (JEM 2010 from JEOL, Akishima, Japan) operating at 200 kV acceleration voltage. TEM images were recorded directly after deposition/annealing and after 3 and 9 weeks. Additional measurements with energy-dispersive X-ray spectroscopy in TEM (TEM-EDX) were taken on AgNW cores and on surrounding shell particles with the same instrument.

## 3. Results and Discussion

### 3.1. Stability of Drop Casted Silver Nanowire Networks Without Polymer Matrix

Figure 2 shows the ageing of AgNW layers after different treatments as change of  $R/R_0$ , where  $R$  is the electrical resistance and

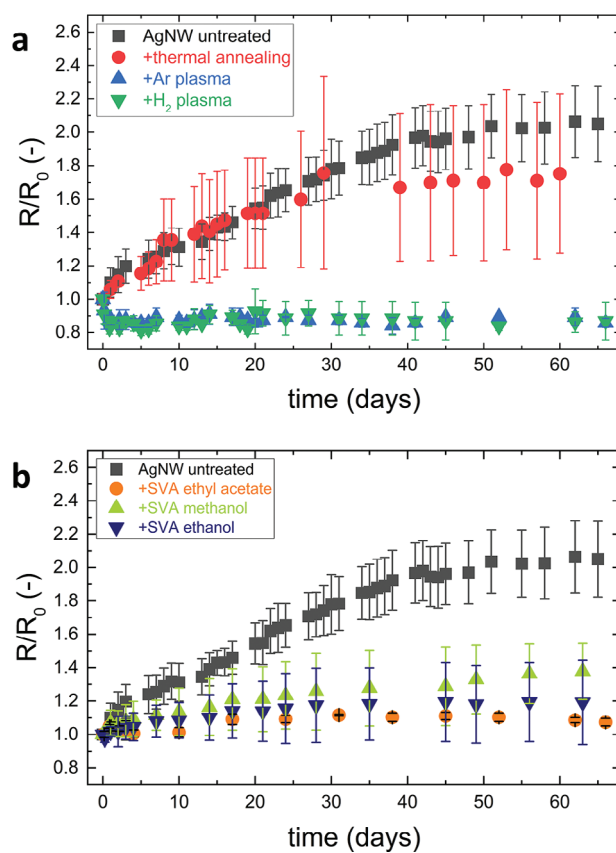


**Figure 2.** Relative change in electrical resistance ( $R/R_0$ ) of drop cast AgNW networks observed over time after different treatments. a) Thermal annealing (150 °C, 30 min) and plasma treatment (30 min, Ar, or  $H_2$  plasma) versus untreated AgNW. b) Solvent vapor annealing (15 min, ethanol, methanol, or ethyl acetate) versus untreated AgNW. Initial resistances  $R_0$  directly after treatment are provided in the Supporting Information file.

$R_0$  the initial resistance measured directly after treatment. The resistance of untreated AgNW networks increased monotonously and was taken as reference. Thermally annealed (150 °C, 30 min) AgNW networks showed similar increase in resistance over time as untreated AgNW (Figure 2a).

The plasma treated samples displayed minor initial drops in  $R/R_0$  to about 0.85 and then retained their resistance for at least two months. This is tentatively attributed to cross-linking of the polymer ligand shell around the AgNW as detailed further below. Noble gas plasmas are known to cause cross-linking in polymers.<sup>[35]</sup> The similarity in trends between both plasma treatments could be because of the low hydrogen content of the  $H_2$  plasma (5 vol%  $H_2$  in Ar).

Solvent vapor annealing with ethanol, methanol or ethyl acetate significantly slowed down the increase in resistance during at least 2 months (Figure 2b). Among the solvents investigated here, ethyl acetate achieved best stability at lowest error margin. As ethyl acetate also dissolves polystyrene it was chosen for the filming of a PS matrix in the investigation of AgNW/PS composites below.

AgNW layers were analyzed by scanning electron microscopy directly after treatments of thermal annealing,  $H_2$  plasma

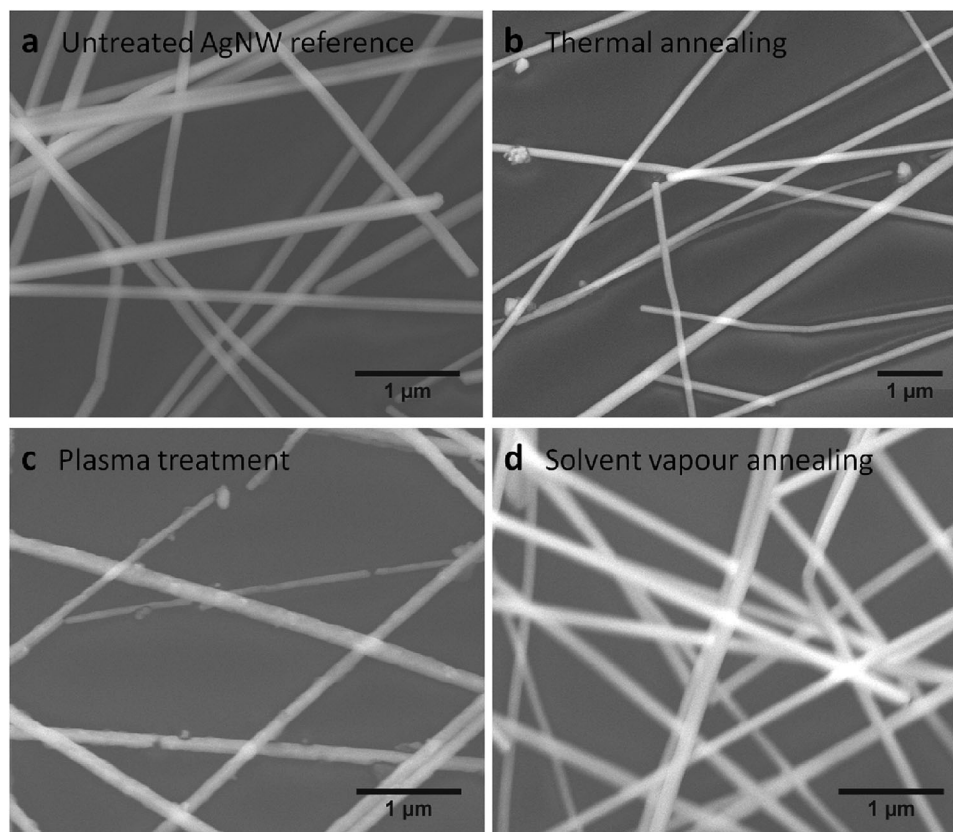


**Figure 3.** SEM micrographs of AgNW layers after different treatments: a) Untreated reference. b) Thermal annealing (150 °C, 30 min). c) Exposure to H<sub>2</sub> plasma (30 min). d) Solvent vapor annealing with ethyl acetate (15 min ethyl acetate).

treatment and solvent vapor annealing (**Figure 3**). When compared to untreated AgNW (**Figure 3a**), the thermally annealed AgNW layers (**Figure 3b**) contained sporadic round grains that indicate a minor breakdown of the AgNW caused by the thermal annealing. A dissimilar type of grains was observed on plasma treated AgNW (**Figure 3c**), where the entire surface of the AgNW appeared to be altered by the treatment. **Figure 3c** solely shows morphological changes caused by plasma exposure. The changes can be explained by the known cross-linking effect of the plasma on the PVP ligand shell.<sup>[35,36]</sup> The particles likely form through Ag sputtering upon local PVP removal. For solvent vapor annealed AgNW (**Figure 3d**) no morphological changes could be identified by SEM. However, focusing was impaired here, presumably because of degassing solvent from the freshly annealed layer.

The morphological ageing of untreated AgNW, solvent-vapor annealed (ethyl acetate) AgNW, and Ar plasma treated AgNW was compared using transmission electron microscopy. **Figure 4** displays transmission electron micrographs of the AgNW directly after deposition and treatment, and after 3 and 9 weeks, respectively.

After 3 weeks of ageing, numerous nanoparticles were found on the surface of the AgNW and in their direct vicinity (**Figure 4**). Over the entire period of investigation, untreated, solvent vapor annealed, and plasma treated AgNW appeared similar in TEM analysis, with no major feature that could be linked to the observed stability in electrical resistance. This suggests that the electrical stabilization happens at positions invisible by TEM

(in between the wires) or through a mechanism that does not change the TEM contrast. The TEM analysis neither supports nor contradicts a potential cross-linking of the PVP shell around the AgNW and does not indicate obvious differences in the rate of structural change between untreated, vapor-annealed, and plasma-treated AgNW. The observed formation of nanoparticles reminds of previous reports such as Elechiguerra et al.,<sup>[19]</sup> who found such nanoparticles to be newly formed crystallites of silver sulphide. On the other hand, pure silver nanoparticles have been found before on macroscopic silver objects<sup>[37]</sup> and PVP has been reported to reduce Ag<sup>+</sup> ions to form silver nanoparticles.<sup>[38,39]</sup>

In the present study, an EDX analysis of the nanoparticles next to the AgNW yielded a low-intensity sulphur peak (**Figure 5b**, indicated by arrow), while the silver peaks of the respective particles had much lower intensity than when measured directly on the AgNW (**Figure 5a**). This indicates that the particles observed here are at least partially silver sulphide. The corrosion of AgNW by sulphidation can be driven by atmospheric H<sub>2</sub>S and water.<sup>[14,25]</sup> Here, the atmospheric influence was revealed by storing an AgNW network in an argon atmosphere. The resistance of this AgNW network did not increase until the argon was exchanged for air after 28 days (**Figure 5c**). The coverage of all AgNW with nanoparticles already after three weeks as observed in TEM (**Figure 4**) does not necessarily exclude the ability of AgNW networks to conduct electricity, despite the lower conductivity of silver sulphide. Mayousse et al.<sup>[25]</sup> noted a

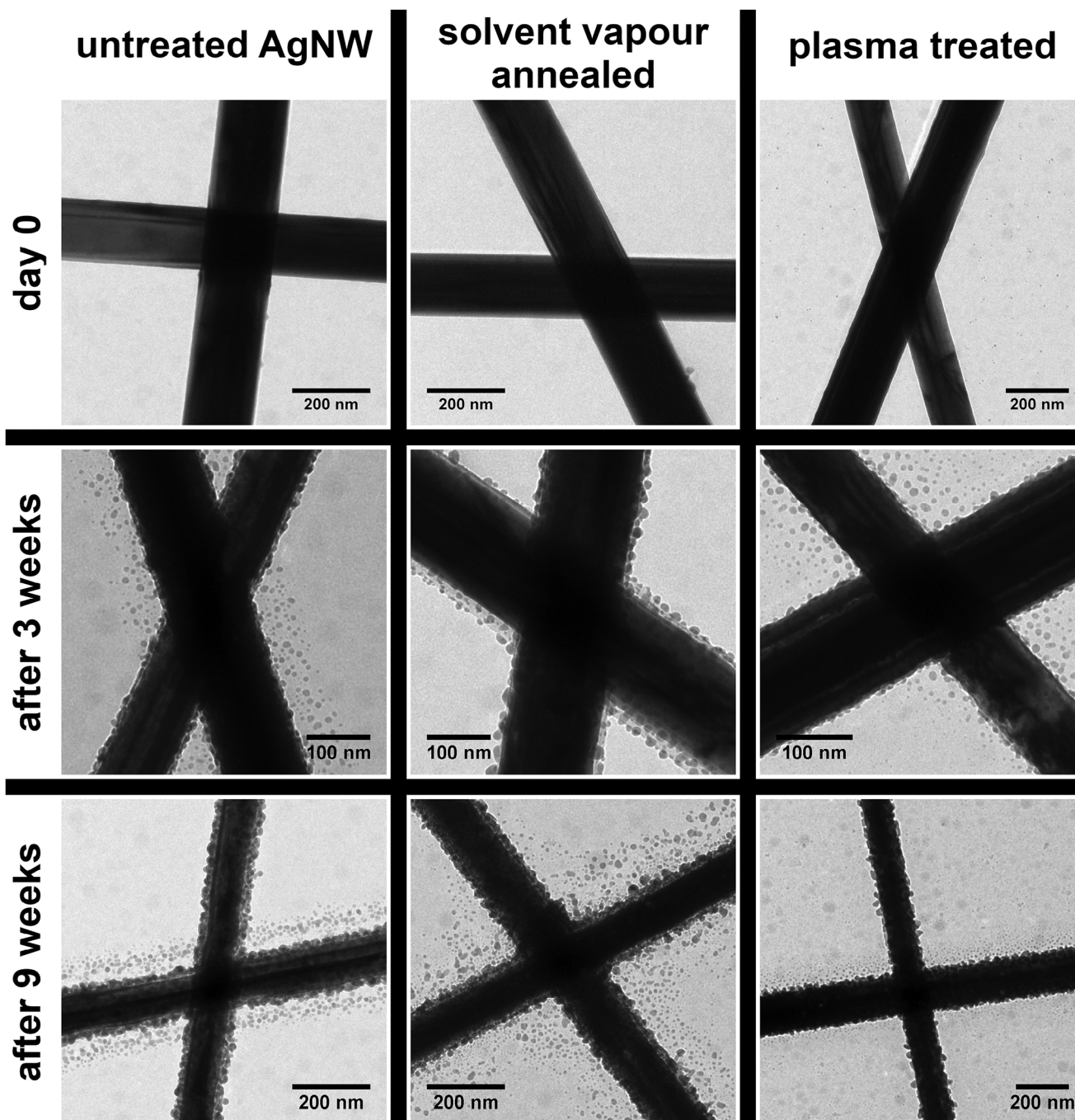


**Figure 4.** Transmission electron micrographs of AgNW junctions for untreated AgNW (left), solvent vapor annealed AgNW (middle, 15 min ethyl acetate) and plasma treated AgNW (right, 30 min. Ar plasma). From top to bottom: AgNW directly after treatment, and 3 or 9 weeks after treatment.

similar observation when investigating silver sulphide nanoparticles formed on AgNW after accelerated corrosion in  $H_2S$  atmosphere.

The stabilizing effects of plasma treatment and solvent vapor annealing on the electrical resistance of AgNW networks (Figure 2) were not caused by changes in the wire network visible in SEM (Figure 3) or TEM (Figure 4). We conclude that the stabilizing mechanism acts at the nanowire junctions, establishing a stable conductive path that does not corrode. The experi-

mental results show that corrosion is caused by components of air, specifically,  $H_2O$  and  $H_2S$ . They pass the ligand shell: PVP is known to be permeable to water.<sup>[40]</sup>

Corrosion of silver nanowires and nanoparticles has been reported to form core-shell structures. We observed such structures in TEM (Figure 4), where silver sulphide shells surrounded the original wires.<sup>[19,20]</sup> The formation of silver nanoparticles that is shown in Figure 4 has been reported before, too, and explained by the dissolution of  $Ag^+$  in adsorbed water<sup>[20]</sup> with subsequent

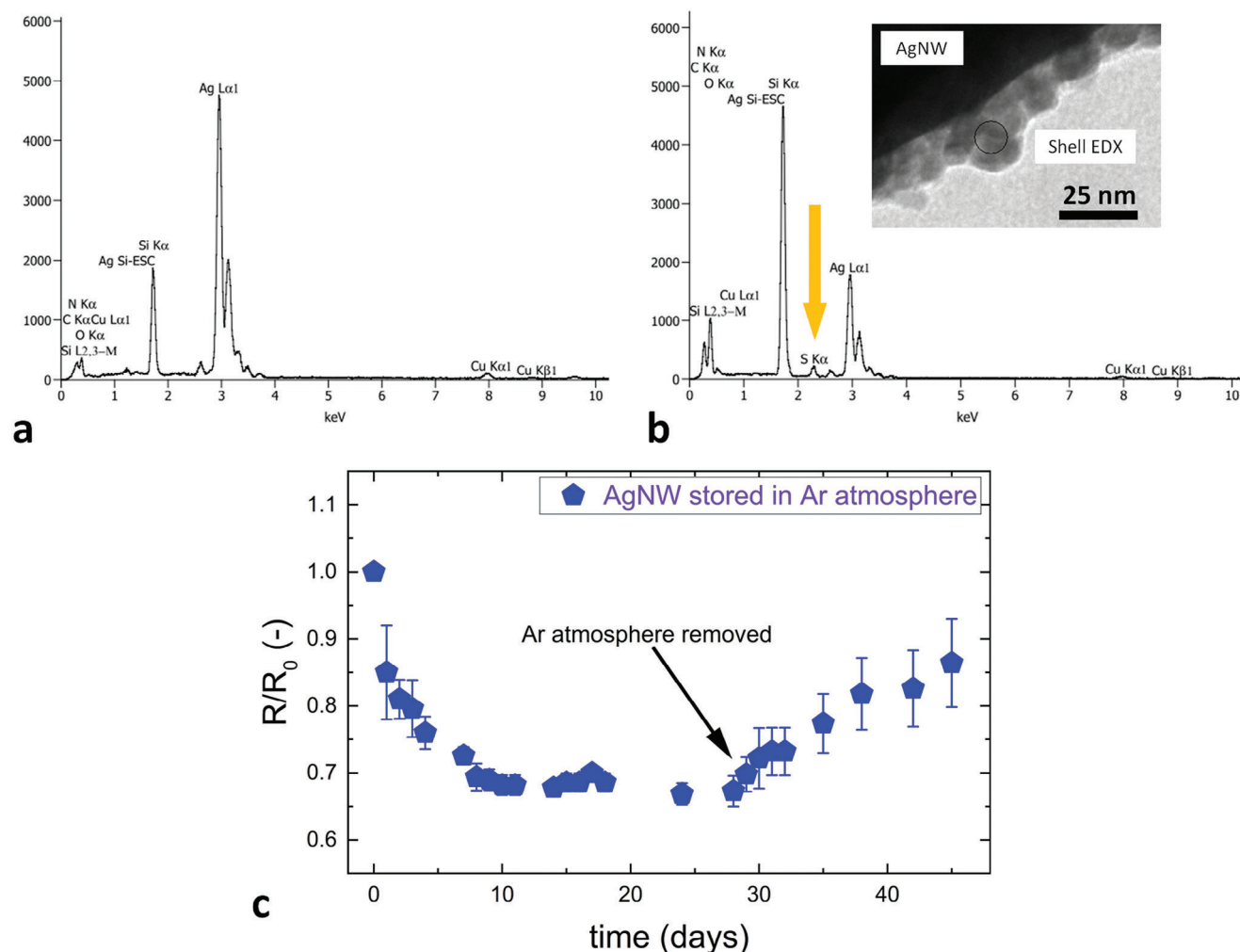


**Figure 5.** a,b) TEM-EDX spectra taken at (a) the centre of an AgNW and b) at a shell particle as indicated in the inset TEM micrograph in (b). The y-axis of (a,b) represents counts. The arrow in (b) highlights the sulphur peak. c) Relative change in electrical resistance over time for AgNW layers stored in Ar atmosphere. Visible resistance increase can be seen after 28 days, when the Ar atmosphere was exchanged for air. Initial resistance  $R_0$  is provided in the Supporting Information file.

reduction by PVP.<sup>[38,39]</sup> The nanoparticles thus formed link by Ag<sub>2</sub>S nanobridges and form conductive connections that are corrosion stable.<sup>[20]</sup> We conclude that such bridges at nanowire junctions explain the observed long-term stability in electrical resistance.

This leaves the question why the stabilization required plasma or solvent vapor. Plasma treatments can cross-link PVP ligand shells,<sup>[35]</sup> solvent vapor annealing induces swelling of the shells.<sup>[41]</sup> We consistently find that PVP absorbed and released solvent by infrared spectroscopy of a vapor annealed PVP film (see the Supporting Information file for details). We conclude that plasma cross-linking or density enhancement by swelling/deswelling enhances wires contact in the junction and enables their bridging by the known Ag<sub>2</sub>S nanobridges. This overall mechanism is illustrated in **Figure 6**. The initial drop in  $R/R_0$  that only occurred for plasma treatment (Figure 2) indicates that cross-linking of the ligand shells in nanowire junctions establishes a closer connection than interpenetration of ligand shells by vapor annealing.

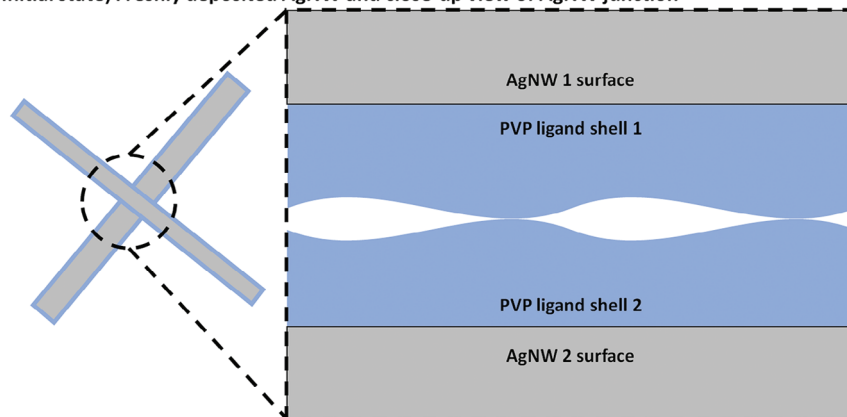
### 3.2. Ageing of AgNW/PS Composite Films

Considering the above stabilizing effect of solvent vapor annealing on AgNW resistance, it is interesting to test how this can be used for creation of polymer matrix composites containing AgNW. Among the solvents investigated above, ethyl acetate performed best (Figure 2b). Ethyl acetate is a good solvent for polystyrene, which is readily available as suspensions of colloidal PS microbeads.

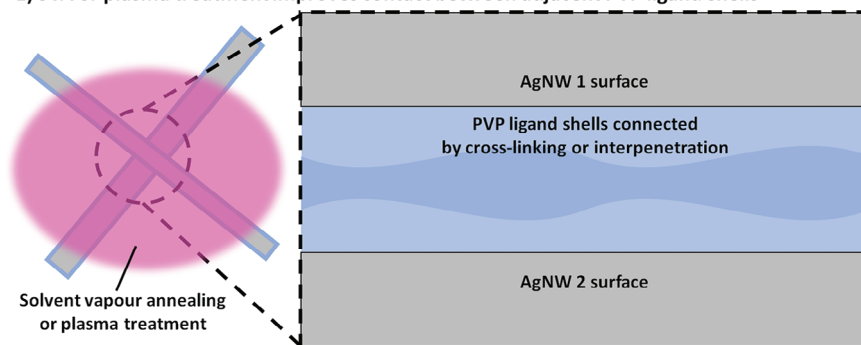
As a proof of concept, we prepared suspensions of AgNW and PS microbeads (diameter 1  $\mu$ m) in isopropanol, drop casted them onto glass substrates and, after drying, subjected the samples to solvent vapor annealing with ethyl acetate. This led to the formation of a PS film from the PS beads, yielding AgNW-containing polymer matrix composites. We compared their relative change in resistance with that of drop casted AgNW without PS, subjected to a similar solvent vapor annealing.

The AgNW/PS films and the AgNW control both displayed a constant  $R/R_0$  over more than two months (**Figure 7**).

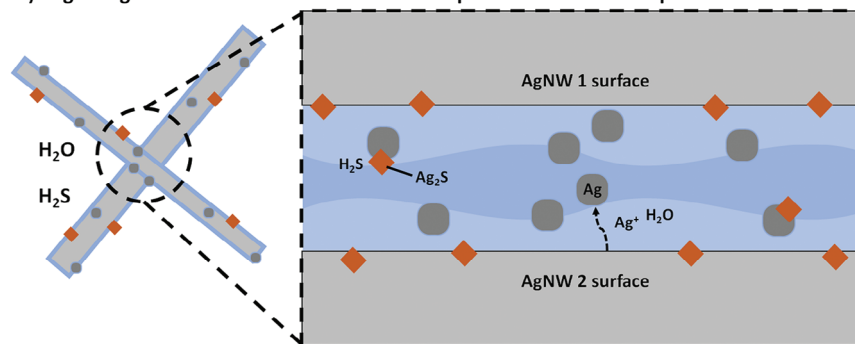
Initial state) Freshly deposited AgNW and close-up view of AgNW junction



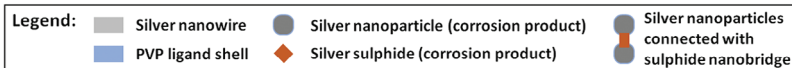
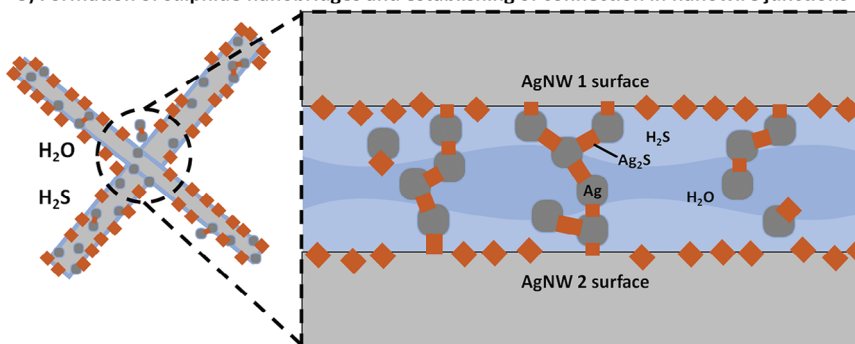
1) SVA or plasma treatment improves contact between adjacent PVP ligand shells



2) Beginning corrosion: Formation of silver nanoparticles and silver sulphide



3) Formation of sulphide nanobridges and establishing of connection in nanowire junctions



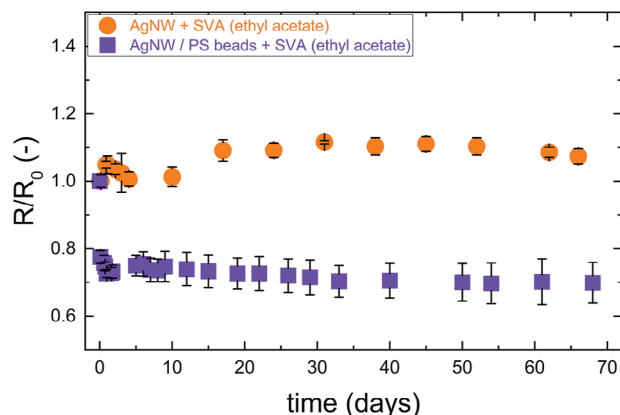


**Figure 7.** Relative change in electrical resistance ( $R/R_0$ ) over time for drop casted samples that were solvent vapor annealed with ethyl acetate. AgNW control (orange circles) versus mixtures of AgNW and PS microbeads (blue squares). Initial resistances  $R_0$  directly after solvent vapor annealing are provided in the Supporting Information file.

We therefore conclude that the solvent vapor treatment is suitable for the processing of stable composites. For the AgNW/PS samples, an initial drop in resistance was observed which is attributed to rearrangement of inter-AgNW distances while the new-formed PS film reaches an equilibrium state after solvent removal.

This new approach for composite formation can potentially be used for printing techniques, since colloidal precursor inks can be deposited more flexibly when compared to viscous polymer solutions or roll-to-roll AgNW film transfer processes. The above proof of concept was done with drop cast samples, but more homogeneous AgNW/PS composite films may be fabricated by deposition with a retreating meniscus approach. To test the feasibility of this, we co-deposited AgNW and PS microbeads (diameter 1  $\mu\text{m}$ ) onto glass substrates by using convection assisted particle assembly (Figure 1b).

Figure 8 shows an exemplary AgNW/PS bead layer after convection-assisted particle assembly and before solvent vapor annealing. The self-assembled bead layers cover the entire displayed area. Bright blue regions are bead multilayers.

The opaque films of AgNW and PS beads were subsequently solvent vapor annealed with ethyl acetate for 15 min, thus creating polymer matrix composites. The transformation of opaque PS bead assemblies into transparent films during solvent vapor annealing is depicted in the inset photographs of Figure 1b. To visualize the merging of PS beads on the microscopic scale, AgNW/PS bead layers with larger bead diameter of 45  $\mu\text{m}$  were prepared by CAPA and exposed to ethyl acetate vapor. With the larger bead diameter, the bead swelling and merging into a film could be observed over a time of 24 h (Figure 9), whereas the film formation took only minutes for the beads with diameter 1  $\mu\text{m}$ .

We now consider the stability of optical properties of these composite layers. After vapor annealing, the freshly prepared

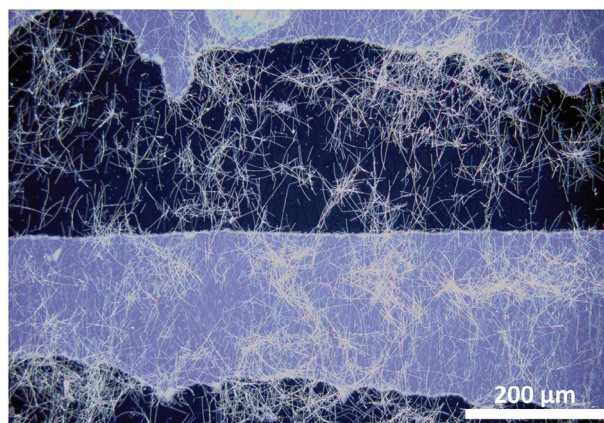


**Figure 8.** Optical micrograph of AgNW/PS bead layer (bead diameter 1  $\mu\text{m}$ ) formed by convection-assisted particle assembly. Bright blue areas are regions with multiple layers of PS microbeads.

AgNW/PS composite films appeared uniform with a slight turbidity except for a few visible AgNW agglomerates (Figure 10a, inset). Figure 10a shows representative UV-vis spectra for a solvent vapor annealed composite film directly after treatment, after 1 week, and after 7 weeks. The combined transmission of composite film and glass substrate at 550 nm was  $63.5 \pm 2.2\%$  directly after SVA and remained stable over the course of 7 weeks. Slight changes of transmittance on the order of less than 5 % that did not follow a systematic trend over time (Figure 10a) are probably measurement artefacts. Transmittance variations between different samples were of the same order. The only distinct feature in the spectra was a broad transmittance minimum centered at  $\approx 440$  nm that did not change over time, i.e., no color change occurred that would be associated with silver corrosion. The transmittance minimum is typical for the surface plasmon resonance of silver nanowires or nanoparticles<sup>[42]</sup> such as the ones observed in TEM (Figure 4).

Figure 10b shows the sheet resistance  $R_{\text{sq}}$  of the composite films over the course of 7 weeks. The sheet resistance of the precursor layers before fusing of PS microbeads was above 40  $\text{M}\Omega$  (limit of measuring device). Solvent vapor annealing reduced this value to an average  $211 \Omega \text{sq}^{-1}$ , which further decreased within the first week and remained stable afterwards. The mean value of sheet resistance after 7 weeks was  $83 \Omega \text{sq}^{-1}$ . The initial resistance drop in the AgNW/PS composites may be associated with changes of inter-AgNW distance during PS film formation and subsequent degassing of the solvent. A similar initial resistance drop was observed for the abovementioned AgNW/PS composites created from drop casted precursors (Figure 7). The protection of the AgNW in the PS matrix composite is probably caused by the solvent vapor annealing with ethyl acetate, following the same effect as observed above for non-embedded AgNW. A protective effect of the PS matrix is unlikely, because similar AgNW/PS composites produced by thermal annealing (150  $^\circ\text{C}$  for

**Figure 6.** Proposed mechanism for the stabilization of electrical resistance that acts at AgNW junctions after solvent vapor annealing or plasma treatment. (1) Improved connectivity between adjacent ligand shells by cross-linking from plasma treatment or interpenetration from solvent vapor annealing. (2) Beginning corrosion: water-assisted formation of silver nanoparticles in the PVP ligand shell. (3)  $\text{H}_2\text{S}$ -assisted formation of  $\text{Ag}_2\text{S}$  nanobridges between silver nanoparticles, leading to conductive connection in nanowire junction.

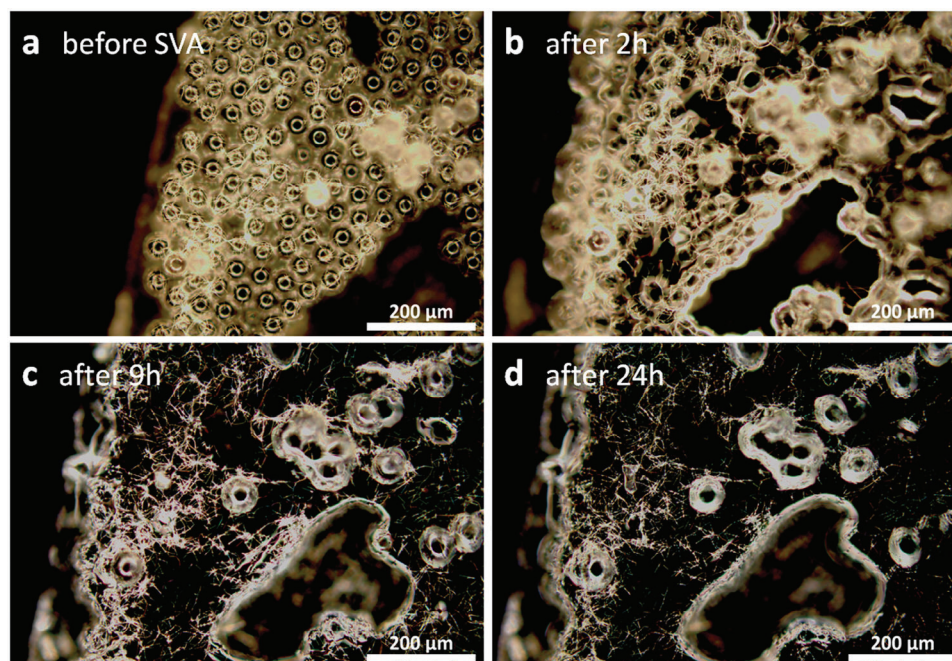


**Figure 9.** Optical micrographs of AgNW/PS bead layer with larger PS beads (45  $\mu\text{m}$  diameter) before (a) and after solvent vapor annealing with ethyl acetate for (b) 2 h, (c) 9 h and (d) 24 h. The larger diameter beads enable visualization of the swelling (b) and subsequent merging (c,d) of PS beads into a film.

30 min) instead of SVA lost their conductivity within less than 2 weeks (Figure S2, Supporting Information).

Although other studies achieved lower sheet resistances (2–20  $\Omega\text{sq}^{-1}$  vs 83  $\Omega\text{sq}^{-1}$  here) and higher transmittances at 550 nm (50–90 % versus 63.5 % here),<sup>[14,15,25,30,32,33]</sup> most did not investigate the long-term stability. One of these studies reported a moderate increase in sheet resistance over time instead.<sup>[25]</sup> The performance of the AgNW/PS composite layers presented here may

be further improved in the future by varying parameters such as nanowire/bead ratio, bead size, deposition rate during CAPA, vapor annealing time and by use of a more sophisticated vapor annealing setup. At this point, we don't yet expect to beat the more established approaches but demonstrate the feasibility of processing AgNW/PS composite films with stable electrical and optical properties by a new approach, where first colloidal precursors (AgNW and PS beads) are co-deposited with convection-assisted

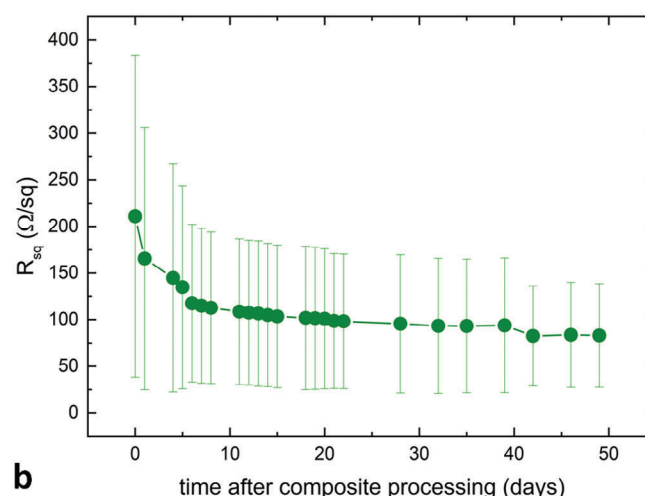
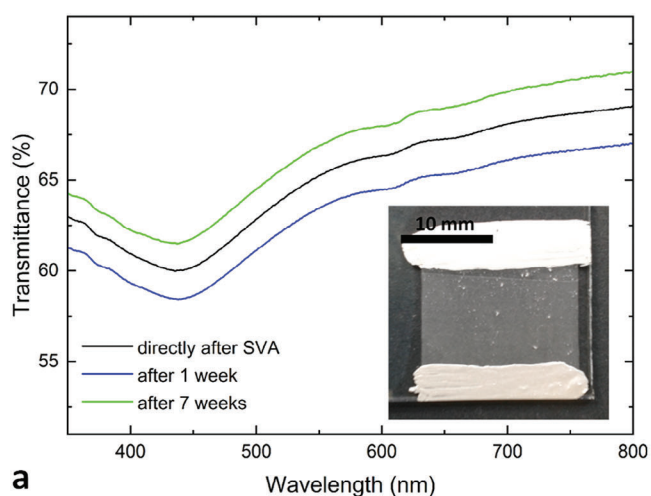


**Figure 10.** (a) UV–vis transmittance of a solvent vapor annealed AgNW/PS composite film on a glass substrate. The minimum at  $\approx 440$  nm is caused by silver nanowires or nanoparticles. Over the course of 7 weeks, no corrosion effects causing color changes could be tracked. Inset: Photograph of a composite film (size 2  $\times$  2 cm) after vapor annealing, with lines of silver paint at top and bottom for electrical contacts. (b) Sheet resistance  $R_{\text{sq}}$  over time for transparent AgNW/PS composite layers produced by solvent vapor annealing.

particle assembly and then the polymer beads are merged into a closed film containing the AgNW by means of solvent vapor annealing. The advantage of this new composite processing method is that it combines the stabilizing effect from solvent vapor annealing with the formation of a polymer matrix that imparts a mechanical stability which is required for many applications. The deposition process of the precursor ink can be adapted to other polymer-solvent pairings. The protective effect of solvent vapor annealing has been demonstrated with other solvents as well (Figure 2b). This process is compatible to printing techniques and enables the manufacturing of composites with prolonged stability of optical and electrical properties while avoiding problems connected to the large viscosities of concentrated polymer solutions<sup>[26,43]</sup> and the cumbersome AgNW network transfer that comes with other two-step processes.<sup>[14,15,32]</sup>

## 4. Conclusion

We compared the stability of untreated AgNW with that of AgNW after thermal, plasma, and solvent vapor treatments, the latter with ethanol, methanol, and ethyl acetate. Here we found a stabilizing effect of plasma treatment and solvent vapor annealing on electrical resistance. This effect is attributed to improved contact of ligand shells in nanowire junctions and subsequent formation of conductive nanoparticle bridges in these junctions. This may be of use for easy processing of AgNW electrodes with prolonged stability. We furthermore showed that solvent vapor annealing can be used to create transparent conductive composite films of AgNW in a PS matrix while maintaining this stabilizing effect. For creation of these composites, we presented a new two-step printing process: Colloidal suspensions carrying AgNW and PS microbeads were deposited by a moving meniscus approach and then solvent vapor annealed with ethyl acetate. The PS beads fused into a polymer film around the AgNW. The resulting composite films had stable sheet resistance and UV-vis transmittance over the course of 7 weeks. The presented process of composite fabrication bears potential for larger-scale printing of stable, transparent electrodes since it is colloid-based and thus avoids typical problems of viscous polymer solutions and is more flexible than roll-to-roll processes.

## Supporting Information

Supporting Information is available from the Wiley Online Library or from the author.

## Acknowledgements

The authors thank Eduard Arzt for his continuing support of the project and Marcus Koch for EDX measurements. TG thanks Ioannis Kanelidis for discussions on infrared spectroscopy. Funding from the German Federal Ministry of Education and Research (BMBF) in the “NanoMatFutur” program is gratefully acknowledged.

Open access funding enabled and organized by Projekt DEAL.

## Conflict of Interest

The authors declare no conflict of interest.

## Data Availability Statement

The data that support the findings of this study are available from the corresponding author upon reasonable request.

## Keywords

plasma, silver nanowires, solvent vapor annealing, stability, transparent conductive material

Received: May 7, 2024

Revised: June 14, 2024

Published online:

- [1] C. Hilsum, *Philos. Transact. A Math. Phys. Eng. Sci.* **2010**, 368, 1027.
- [2] J. Müller, B. Rech, J. Springer, M. Vanecek, *Sol. Energy* **2004**, 77, 917.
- [3] Y. Jin, Y. Sun, K. Wang, Y. Chen, Z. Liang, Y. Xu, F. Xiao, *Nano Res.* **2018**, 11, 1998.
- [4] B.-R. Yang, G.-S. Liu, S.-J. Han, W. Cao, D.-H. Xu, J.-F. Huang, J.-S. Qiu, C. Liu, H.-J. Chen, *J. Soc. Inf. Disp.* **2016**, 24, 234.
- [5] L. Lian, D. Dong, S. Yang, B. Wei, G. He, *ACS Appl. Mater. Interfaces* **2017**, 9, 11811.
- [6] T. Minami, *Thin Solid Films* **2008**, 516, 5822.
- [7] D. Langley, G. Giusti, C. Mayousse, C. Celle, D. Bellet, J.-P. Simonato, *Nanotechnology* **2013**, 24, 452001.
- [8] J.-W. Liu, J.-L. Wang, Z.-H. Wang, W.-R. Huang, S.-H. Yu, *Angew. Chem., Int. Ed. Engl.* **2014**, 53, 13477.
- [9] S. De, J. N. Coleman, *MRS Bull* **2011**, 36, 774.
- [10] T. Tokuno, M. Nogi, M. Karakawa, J. Jiu, T. T. Nge, Y. Aso, K. Suganuma, *Nano Res.* **2011**, 4, 1215.
- [11] A. Bhatt, Á. Mechler, L. Martin, A. Bond, *J. Mater. Chem.* **2007**, 17, 2241.
- [12] Y. Sun, Y. Yin, B. Mayers, T. Herricks, Y. Xia, *Chem. Mater.* **2002**, 14, 4736.
- [13] S. De, T. M. Higgins, P. E. Lyons, E. M. Doherty, P. N. Nirmalraj, W. J. Blau, J. J. Boland, J. N. Coleman, *ACS Nano* **2009**, 3, 1767.
- [14] H.-G. Im, J. Jin, J.-H. Ko, J. Lee, J.-Y. Lee, B.-S. Bae, *Nanoscale* **2014**, 6, 711.
- [15] G.-S. Liu, Y. Xu, Y. Kong, L. Wang, J. Wang, X. Xie, Y. Luo, B.-R. Yang, *ACS Appl. Mater. Interfaces* **2018**, 10, 37699.
- [16] A. Madeira, M. Plissonneau, L. Servant, I. Goldthorpe, M. Tréguer-Delapierre, *Nanomaterials* **2019**, 9, 899.
- [17] J. Li, S. Qi, J. Liang, L. Li, Y. Xiong, W. Hu, Q. Pei, *ACS Appl. Mater. Interfaces* **2015**, 7, 14140.
- [18] J. Idier, W. Neri, C. Labrugère, I. Ly, P. Poulin, R. Backov, *Nanotechnology* **2016**, 27, 105705.
- [19] J. Elechiguerra, L. Larios-Lopez, C. Liu, D. Garcia-Gutierrez, A. Camacho-Bragado, M. Yacaman, *Chem. Mater.* **2005**, 17, 6042.
- [20] C. Levard, B. Reinsch, F. M. Michel, C. Oumahi, G. Lowry, G. E. Brown, *Environ. Sci. Technol.* **2011**, 45, 5260.
- [21] D. Langley, M. Lagrange, G. Giusti, C. Jiménez, Y. Bréchet, N. Nguyen, D. Bellet, *Nanoscale* **2014**, 6, 13535.
- [22] K. Zilberberg, F. Gasse, R. Pagui, A. Polywka, A. Behrendt, S. Trost, R. Heiderhoff, P. Görrn, T. Riedl, *Adv. Funct. Mater.* **2014**, 24, 1671.
- [23] Y. Ahn, Y. Jeong, Y. Lee, *ACS Appl. Mater. Interfaces* **2012**, 4, 6410.
- [24] J. Liang, L. Li, K. Tong, Z. Ren, W. Hu, X. Niu, Y. Chen, Q. Pei, *ACS Nano* **2014**, 8, 1590.
- [25] C. Mayousse, C. Celle, A. Fraczkiewicz, J.-P. Simonato, *Nanoscale* **2015**, 7, 2107.
- [26] K. Wang, Y. Jin, B. Qian, J. Wang, F. Xiao, *J. Mater. Chem.* **2020**, 8, 4372.

- [27] L. Malaquin, T. Kraus, H. Schmid, E. Delamarche, H. Wolf, *Langmuir* **2007**, *23*, 11513.
- [28] B. Prevo, D. Kuncicky, O. Velev, *Colloids Surf., A* **2007**, *311*, 2.
- [29] L. Yang, T. Zhang, H. Zhou, S. C. Price, B. J. Wiley, W. You, *ACS Appl. Mater. Interfaces* **2011**, *3*, 4075.
- [30] C. Gong, J. Liang, W. Hu, X. Niu, S. Ma, H. T. Hahn, Q. Pei, *Adv. Mater.* **2013**, *25*, 4186.
- [31] P. Lee, J. Lee, H. Lee, J. Yeo, S. Hong, K. H. Nam, D. Lee, S. S. Lee, S. H. Ko, *Adv. Mater.* **2012**, *24*, 3326.
- [32] M. Miller, J. Kane, A. Niec, R. Carmichael, T. Carmichael, *ACS Appl. Mater. Interfaces* **2013**, *5*, 10165.
- [33] X.-Y. Zeng, Q.-K. Zhang, R.-M. Yu, C.-Z. Lu, *Adv. Mater.* **2010**, *22*, 4484.
- [34] T. Kraus, Assembly and Printing of Micro and Nano Objects, PhD Thesis, ETH Zürich, xx xx **2007**.
- [35] E. M. Liston, *J. Adhes.* **1989**, *30*, 199.
- [36] H. Zhang, L. Sang, Z. Wang, Z. Liu, L. Yang, Q. Chen, *Plasma Sci. Technol.* **2018**, *20*, 063001.
- [37] R. Glover, J. Miller, J. Hutchison, *ACS Nano* **2011**, *5*, 8950.
- [38] Z. Zhang, B. Zhao, L. Hu, *J. Solid State Chem.* **1996**, *121*, 105.
- [39] C. Wu, B. P. Mosher, K. Lyons, T. Zeng, *J. Nanosci. Nanotechnol.* **2010**, *10*, 2342.
- [40] R. J. Cranford, H. Darmstadt, J. Yang, C. Roy, *J. Membr. Sci.* **1999**, *155*, 231.
- [41] T.-H. Yang, J. Ahn, S. Shi, D. Qin, *ACS Nano* **2021**, *15*, 14242.
- [42] J. Mock, M. Barbic, D. Smith, D. Schultz, S. Schultz, *J. Chem. Phys.* **2002**, *116*, 6755.
- [43] Y. Jin, D. Deng, Y. Cheng, L. Kong, F. Xiao, *Nanoscale* **2014**, *6*, 4812.